Tree-Ring Reconstruction of Single-Day Precipitation Totals over Eastern Colorado

Ian M. Howard *and* David W. Stahle
Department of Geosciences, University of Arkansas, Fayetteville, Arkansas

https://doi.org/10.1175/MWR-D-19-0114.1
Received: 15 April 2019
Final Form: 24 October 2019
Published Online: 8 January 2020

Abstract

Mean daily to monthly precipitation averages peak in late July over eastern Colorado and some of the most damaging Front Range flash floods have occurred because of extreme 1-day rainfall events during this period. Tree-ring chronologies of adjusted latewood width in ponderosa pine from eastern Colorado are highly correlated with the highest 1-day rainfall totals occurring during this 2-week precipitation maximum in late July. A regional average of four adjusted latewood chronologies from eastern Colorado was used to reconstruct the single wettest day observed during the last two weeks of July. The regional chronology was calibrated with the CPC 0.25° × 0.25° Daily U.S. Unified Gauge-Based Analysis of Precipitation dataset and explains 65% of the variance in the highest 1-day late July precipitation totals in the instrumental data from 1948 to 1997. The reconstruction and instrumental data extend fully from 1779 to 2019 and indicate that the frequency of 1-day rainfall extremes in late July has increased since the late eighteenth century. The largest instrumental and reconstructed 1-day precipitation extremes are most commonly associated with the intrusion of a major frontal system into a deep layer of atmospheric moisture across eastern Colorado. These general synoptic conditions have been previously linked to extreme localized rainfall totals and widespread thunderstorm activity over Colorado during the summer season. Chronologies of adjusted latewood width in semiarid eastern Colorado constitute a proxy of weather time-scale rainfall events useful for investigations of long-term variability and for framing natural and potential anthropogenic forcing of precipitation extremes during this 2-week precipitation maximum in a long historical perspective.

Keywords: North America; Paleoclimate

Corresponding author: Ian M. Howard, ihowardksu@gmail.com

Tree-ring reconstruction of single day precipitation totals over eastern Colorado

Ian M. Howard (corresponding author), Department of Geosciences, University of Arkansas, Fayetteville, AR 72701 ihowardksu@gmail.com

David W. Stahle, Department of Geosciences, University of Arkansas, Fayetteville, AR 72701 dstahle@uark.edu

January 23, 2020

Manuscript accepted for publication in *Monthly Weather Review*, February issue, 2020

Abstract

Mean daily to monthly precipitation averages peak in late-July over eastern Colorado and some of the most damaging Front Range flash floods have occurred because of extreme one day rainfall events during this period. Tree-ring chronologies of adjusted latewood width in ponderosa pine from eastern Colorado are highly correlated with the highest one-day rainfall totals occurring during this midsummer precipitation maximum. A regional average of four adjusted latewood chronologies from eastern Colorado was used to reconstruct the single wettest day observed during the last two weeks of July. The regional chronology was calibrated with the CPC 0.25°x0.25° Daily U.S. Unified Gauge-Based Analysis of Precipitation dataset and explains 65% of the variance in the highest one-day midsummer precipitation totals in the instrumental data from 1948-1997. The reconstruction and instrumental data extend fully from 1779-2019 and indicate that the frequency of one-day rainfall extremes in midsummer has increased since the late-18th century. The largest instrumental and reconstructed one-day precipitation extremes in midsummer are most commonly associated with the intrusion of a major frontal system into a deep layer of atmospheric moisture across eastern Colorado. These general synoptic conditions have been previously linked to extreme localized rainfall totals and widespread thunderstorm activity over Colorado in midsummer. Chronologies of adjusted latewood width in semiarid eastern Colorado constitute a proxy of weather timescale rainfall events useful for investigations of long-term variability and for framing natural and potential anthropogenic forcing of midsummer precipitation extremes in a long historical perspective.

Key words: midsummer rainfall maximum; single day rainfall extremes, flash flooding, eastern Colorado, adjusted latewood width, ponderosa pine, dendrometeorology

1. Introduction

Extreme midsummer rainstorms have caused some of the most damaging flash floods to impact the Colorado Front Range, including the catastrophic floods at Big Thompson Canyon on July 31, 1976 (Maddox et al. 1978), and at Spring Creek near Fort Collins on July 27-28, 1997 (Doesken and Mckee 1998). Heavy precipitation and major flash flooding in Colorado can occur throughout the year (Mckee and Doesken 1997), famously including Denver's "flood of record" in June 1965 (Matthai 1969) and the flooding of September 2013 over northern Colorado (Gochis et al. 2015). But the Front Range and High Plains of Colorado are especially vulnerable to extreme precipitation and flash flooding in midsummer when the advection of subtropical moisture and relatively weak upper-level steering winds can result in slow-moving thunderstorms capable of producing significant hourly and daily rainfall totals (Maddox et al. 1978; McKee and Doesken 1997; Cotton et al. 2003). The frequency and intensity of extreme rainfall events appear to have increased over the United States since 1901 (Kunkel et al. 2013; Wuebbles et al. 2017) and the positive trend has been most pronounced in summer (Karl and Knight 1998). However, there is less evidence for changes to extreme precipitation over Colorado (Hoerling et al. 2013; Lukas et al. 2014; Mahoney et al. 2018). While global climate model simulations suggest that the frequency and magnitude of daily rainfall extremes may increase with unabated anthropogenic global warming (Kunkel et al. 2013; Wuebbles et al. 2017; Mahoney et al. 2018), there is large uncertainty associated with changes in extreme summer rainfall events in Colorado (Alexander et al. 2013). Historical documentary evidence, early instrumental observations, and potentially exactly-dated wood anatomical or sub-annual tree-ring width data might provide a longer historical perspective on midsummer rainfall extremes prior to the onset of heavy anthropogenic weather and climate forcing.

Climate sensitive tree-ring chronologies have been widely used to reconstruct growing season precipitation and the Palmer Drought Severity Index (PDSI; Palmer 1965; Stahle and Cleaveland 1992; Fritts 2001; Cook et al. 2007). Douglass (1920) described tree growth as a response to integrated climate conditions "distributed throughout the year." The correlation between annual precipitation totals and tree-ring chronologies can in fact be so high that they have been referred to as "integrating pluviometers" (Blasing and Fritts 1976). Because tree growth tends to use soil moisture accumulated during or even preceding the growing season, it has not been possible to develop estimates of daily timescale weather phenomena on a continuous year-by-year basis extending back into prehistory using total ring-width chronologies. Weather extremes associated with severe growing season freeze events (LaMarche and Hirshboeck 1984; Stahle 1990; Bräuning et al. 2016; Barbosa et al. 2019) and mid-growing season weather reversals (Villalba and Veblen 1996; Fritts 2001; Edmondson et al. 2010) may induce distinctive anatomical evidence in the xylem cells of living trees. The meteorological significance of these so-called frost and false ring chronologies can be demonstrated during the instrumental period and then used to infer the history of these episodic events during the pre-instrumental era. But weather sufficiently extreme to cause anatomical damage to tree rings is infrequent, so the derived event chronologies tend to be highly discontinuous in time.

In this article we describe the strong correlation between the single wettest 24-hour period during late-July (July 19-August 1) and a regional tree-ring chronology based on the last-formed latewood cells of ponderosa pine (*Pinus ponderosa)*, the so-called "adjusted latewood width" chronology (hereafter referred to as simply "latewood," "adjusted latewood," or "LWa"). The late-July interval is climatologically the wettest time of the year over eastern Colorado based

on average two-week precipitation totals. The regional adjusted latewood chronology is also highly correlated with total monthly precipitation in July over an area of eastern Colorado [37.75°-39.75°N, 105°-103°W], but higher correlations are computed when the latewood data are compared only with the wettest 24-hour rainfall interval during late-July. The exact Julian date of these 24-hour rainfall extremes vary from year to year, but for the available ponderosa pine chronologies they are restricted to the period from July 19-August 1. These largest rainfall days also constitute the majority of the full two-week total precipitation for late-July in eastern Colorado, and we use the strong single-day signal in adjusted latewood width data to reconstruct the wettest 24-hour totals each year from 1779 to 1997. These "dendrometeorological" rainfall proxies are then used along with instrumental observations to describe the synoptic meteorology and long-term changes in midsummer rainfall extremes, placing them in the context of natural weather and climate variability since the late-18th century.

Warm season precipitation climatology in eastern Colorado

Warm season (April-September) precipitation contributes over 70% of the annual total in the semiarid Front Range and adjacent High Plains of eastern Colorado (Mahoney et al. 2015). However, a substantial fraction of the April-September total tends to occur during two periods when daily precipitation rates are highest (Fig. 1). Averaged across the eastern Colorado study region (black box on the map of the United States in Fig. 1), these spring (May) and midsummer (late-July) rainfall maxima are separated by a drier early-summer period that reaches a minimum on Julian day 182 (July 1). For much of eastern Colorado the timing of the annual precipitation maximum usually occurs in midsummer, but in the northern parts of the study region the highest daily precipitation rates tend to occur in late-spring. The gridded daily data may also

underestimate the spring precipitation peak because the daily totals are calculated for the period 1200-1200 UTC (Chen et al. 2008) and maximum 24-hour precipitation during the spring season may extend across over two days more often than in midsummer.

Higher daily precipitation rates in spring are generally associated with the passage of synoptic-scale storm systems that transport moisture from the Gulf of Mexico northwestward into eastern Colorado. The larger secondary peak in late-July can partly be attributed to the Great Plains low-level jet that advects Gulf moisture on the western sector of a persistent ridge that commonly develops in summer over the central United States (Tang and Reiter 1984). The low pressure system related to the North American Monsoon system can also funnel moist mid-to-upper level air as far northward as Colorado and southern Wyoming, particularly during late-July and early-August (Hales 1974; Tang and Reiter 1984). Pulses of sub-tropical moisture from these two sources, combined with factors such as the topography of the Rocky Mountains, daytime heating of the land surface, and the passage of weak synoptic disturbances embedded in the upper-level flow, result in localized convective thunderstorms that are a near daily occurrence from early summer through as late as September (McKee and Doesken 1997). Certain configurations of atmospheric circulation over the United States, combined with additional forcing from strong frontal systems and upper-level synoptic shortwaves, can enhance the advection of sub-tropical moisture and create thermodynamic conditions that have been responsible for some of the largest hourly and daily rainfall totals recorded in Colorado during the midsummer period.

2. Data and Methods

a. Daily rainfall data

The gridded daily precipitation data used in this study were acquired from the National Oceanic and Atmospheric Administration (NOAA) Climate Prediction Center (CPC) 0.25°x0.25° Daily U.S. Unified Gauge-Based Analysis of Precipitation dataset (Chen et al. 2008). The gridded daily data were calculated using the optimal interpolation algorithm described by Xie et al. (2007), which utilizes a dense network of observing sites to calculate daily precipitation values on a 0.25° latitude by 0.25° longitude grid extending from 1948-2005, with real time observations provided from 2006-present. The daily totals at each grid point are based on the 24 hour accumulation of precipitation ending at 1200 UTC of the current day. The daily precipitation data were extracted for an area of eastern Colorado (black box in Fig. 2). This 2.0°x2.0° region was selected because the daily, biweekly, and monthly precipitation totals calculated for this study area tended to have the highest correlation with the tree-ring data compared to other domains. Rarely do the individual grids points in the eastern Colorado study region contain zero values due to the nature of the interpolated data. For the purposes of this study, we treated daily precipitation values of less than 1mm as zero at each grid point.

Daily precipitation totals from 40 selected observation stations in eastern Colorado in the Global Historical Climatology Network (GHCN) from the National Climatic Data Center (NCDC) were also used for analyses with the gridded daily data and tree-ring chronologies (Fig. 2). These 40 stations were selected based on their location within or near the eastern Colorado study region (Fig. 2), and the availability of at least 25 years of continuous observations of late-July daily precipitation totals. Daily atmospheric data derived from the NCEP/NCAR Reanalysis project (Kalnay et al. 1996) were used to identify synoptic-scale circulation features associated with the largest reconstructed one-day rainfall totals over eastern Colorado. Because many of the station records begin after 1940, we restrict our analyses of the individual station

155 observations to the period 1940-2019. Anomalies in the reanalysis data were calculated relative
156 to the 1981-2010 climatology.
157
158 **b. Eastern Colorado study region and adjusted latewood chronology development**
159 The range of ponderosa pine extends sparsely eastward from the Rocky Mountain Front
160 Range into the Black Forest region of eastern Colorado. Native stands with old trees can
161 occasionally be found on fire-protected escarpments and on certain higher elevation
162 microenvironments (Wells 1965). Several annual ring-width chronologies of ponderosa pine
163 have been previously developed in the study region and used to reconstruct spring PDSI and
164 streamflow (Woodhouse and Brown 2001; Woodhouse and Lukas 2006). The annual growth
165 ring for many temperature North American tree species is made up of several earlywood (EW)
166 and latewood (LW) xylem cells that can be separately identified and measured each year. We
167 remeasured four of these tree-ring collections for EW, LW, and total ring width (RW), and then
168 computed the adjusted latewood width (LWa) chronologies for Black Forest East (BFE),
169 Jefferson County (JFU), Ridge Road (RIR), and Turkey Creek (TCU; open circles in Fig 2).
170 These four sites are all located east of the continental divide, and range in elevation from 1800
171 (BFE) to 1965 meters (JFU).
172 The following steps were used to compute the regional adjusted latewood width
173 chronology for the eastern Colorado study region:
174 1. The previously collected and dendrochronologically dated core samples from four sites in
175 Colorado (approximately 150 individual core specimens) were re-measured for EW, LW, and
176 RW with a stage micrometer to 0.001 mm precision using the protocols outlined by Stahle et al.
177 (2009).

2. Tree-ring chronologies of EW, LW, and RW width were computed for each site using the signal free method of standardization (Melvin and Briffa 2008; Cook et al. 2014). Power transformed ring-width indices were calculated as residuals from the fitted growth curve, and then averaged into the mean index chronology using the biweight robust mean (Cook 1985; Hoaglin et al. 2000).

3. Because the correlation between the EW and LW chronologies from a given site can be quite high (Torbenson et al. 2016), it is necessary to remove the dependency of LW on EW growth in order to derive separate estimates of summer precipitation from LW not dominated by spring climate and tree growth (Meko and Baisan 2001). These so-called adjusted latewood width chronologies are calculated via regression techniques (Meko and Baisan 2001) and represent the tree growth variability that is independent of the EW. Therefore, these chronologies most likely represent the final latewood xylem cells of the annual ring formed at the end of the growing season. Adjusted latewood width chronologies for eastern Colorado were calculated using the Kalman Filter (Welch and Bishop 2006) to allow for potential time-dependent variations in the relationship between EW and LW. In the case of North American conifers, LWa chronologies tend to be correlated *only* with summer precipitation totals (Meko and Baisan 2001; Stahle et al. 2009; Griffin et al. 2011, 2013; Crawford et al. 2015; Dannenberg and Wise 2016; Howard et al. 2019). However, this research in semiarid eastern Colorado indicates that LWa chronologies of ponderosa pine may be dominated by rainfall variability considerably shorter than the full summer season, in this case even at the daily timescale.

4. The variance for the four LWa chronologies had to be stabilized (Meko 1981) to account for changes in tree vigor with age and the declining sample size of dated ring width series in the beginning years of each chronology. A smoothing spline with a 50% frequency response equal

201 to 100-years (Cook and Peters 1981) was fit to the absolute values of the annual LWa indices,
202 and the ratios of the fitted spline to the absolute values were computed. The sign was then
203 restored, and the mean added back to each annual value to produce the variance-stabilized LWa
204 chronologies (Meko 1981; Cook and Krusic 2005).
205 5. The annual values for all four LWa chronologies were squared to increase skewness and
206 better represent the distribution of the daily precipitation data for eastern Colorado.
207 6. The four adjusted latewood chronologies were then averaged for each year in common from
208 1779-1997 to produce the regional chronology used for the reconstruction of daily rainfall
209 extremes in midsummer.
210
211 **c. Daily precipitation response of the regional adjusted latewood chronology**
212 The gridded daily precipitation data were used to identify the highest correlation between
213 the adjusted latewood width chronology and various daily to seasonal precipitation totals in
214 eastern Colorado. The calculation of these daily to near-annual response profiles is summarized
215 as follows:
216 1. The daily precipitation data were regionally averaged for the 72 grid points in eastern
217 Colorado. The regionally average daily data were then totaled for all possible intervals from 2 to
218 365 days (n = 364) throughout the year (e.g., the 2-day total for January 1 represents
219 precipitation summed from December 31 – January 1; December 31 is equal to the two day total
220 for December 30 - 31). This produces a total of 132,860 annual time series (364 possible
221 intervals multiplied by 365 days).

2. The accumulated precipitation for all intervals from 2- to 365-days were correlated with the adjusted latewood chronology for every day of the year, and the correlation coefficients were calculated for all 365 Julian days.

3. All possible 1- to 31-day intervals during the year were used to identify the wettest single day in the given interval, producing a total of 11,315 annual time series (31 intervals multiplied by 365 days). Using the 14-day interval in late-July as an example (i.e., July 19 to August 1), the largest single day total in 1959 for this interval occurred on July 26 (Fig. 3a). The value of 1.35 mm represents the regionally averaged value and the wettest 24-hour total for the 14-day period from July 19-August 1, 1959. For the year 1985, the highest 24-hour rainfall total in late-July was 25.67 mm and occurred on July 19 (Fig. 3b). Note that for correlation with the tree-ring data, the optimal period for the wettest single day in all possible intervals turned out to be only 14-days long in late-July (Fig. 4a).

4. The wettest single day in every possible 14-day interval during the year was correlated with the regional LWa chronology, and the correlation coefficients were plotted by Julian day (red line in Fig. 4a). For all possible 365 Julian days, the wettest day could be the same day for overlapping 14-day intervals. But for any given two-week interval there was just one wettest day in that 14-day period.

5. The regional LWa correlation with regionally averaged precipitation totals *accumulated* for 7, 14, 21, 28, 35, 42, 49, and 56 days was also plotted by Julian day to compare with the correlations with the wettest single day totals (gray lines in Fig. 4a)

6. The various 2- to 365-day accumulated precipitation totals were also correlated with the regional EW, LW, and RW chronologies to compare their seasonal response with the adjusted latewood chronology (Fig. 5).

d. Tree ring reconstruction of one-day precipitation extremes in midsummer

Because the regional LWa chronology was best correlated with the wettest single day in the last two weeks of July (July 19-August 1), it was calibrated with a time series based on the wettest 24-hour period from July 19 to August 1 for the common interval 1948-1997. A secondary instrumental time series of the wettest single day in late-July was also extracted for eastern Colorado based on the grid point that contained the largest precipitation value each year from July 19-August 1. The regionally averaged time series was rescaled to this secondary series using simple linear regression, and the fitted values represent 24 hour precipitation totals similar to the mean and magnitude of extreme rains that occur at localized scales over eastern Colorado. Rescaling the time series in this manner also prevented negative values from being estimated in the tree-ring reconstruction.

Since the tree-ring data end in 1997, the reconstruction was calibrated on the 50-year period from 1948-1997. Separate calibration and validation experiments were performed for two sub-periods from 1948-1972 and 1973-1997. The regional latewood chronology was first calibrated with the instrumental series using regression from 1973-1997, and the instrumental data from 1948-1972 were withheld for independent validation of the reconstruction. The regional LWa chronology was also calibrated on the earlier period, and the estimates were then independently validated on the later period. Because the coefficients of these two regression-based calibration models are similar, the final reconstruction was based on the full time period in common to the instrumental rainfall and adjusted latewood width data, 1948-1997. The variance lost in the regression was restored to the reconstructions from 1779-1997 and the instrumental values were then appended to the estimates to complete the full reconstructed and instrumental time series from 1779 to 2019.

3. Results

The regional adjusted latewood chronology is significantly correlated with July precipitation totals for eastern Colorado ($r = 0.68$, $p < 0.0001$), but the correlation with the time series of the highest one-day rainfall amount during the last two weeks of July is actually much stronger ($r = 0.81$, $p < 0.0001$; Fig. 4a). The correlation coefficients computed between the regional LWa chronology and the single highest daily precipitation total for all possible 14-day intervals during the year are plotted in Figure 4a (the correlation for Julian day 1 is with the highest daily total between December 19 and January 1). These correlations peak on Julian day 213 when the Pearson correlation with the wettest day in the two week interval reaches $r = 0.81$ (Spearman correlation is $r = 0.73$; not shown). Note the sharp increase in correlations at Julian day 200, indicating that this regional LWa chronology begins to be significantly correlated with the heaviest one-day rainfall totals beginning in the second week of July, even though the peak response is during the interval from Julian day 200-213, or July 19-August 1 (Fig. 4a). When the same method is applied using the 40 individual weather stations (black dots in Fig. 2), the highest correlation is also with the wettest daily total identified from July 19-August 1 each year ($r = 0.77$; not shown). The overall highest correlation is in fact with the single wettest day identified at an individual grid cell each year ($r = 0.83$; not shown) instead of a regional average. However, the regionally averaged time series was used in calibration with the tree-ring data since this variable better represents how much it rained over eastern Colorado on a given day, and thus deemed more appropriate to use in calibration with a regionally averaged tree-ring chronology.

For comparison with the response to one-day totals in midsummer, the LWa chronology was also correlated with precipitation totaled for all possible 7-day to 56-day intervals during the year (Fig. 4a). The highest correlation with these various weekly to monthly precipitation totals

291 reaches 0.78 for the 14-day period also ending on Julian day 213, so that roughly 60% of the
292 LWa variance might be explained by the two-week rainfall *total* in late-July for a regional
293 average compared with 65% of the variance associated with the highest one-day total during the
294 same period. Correlation with the LWa chronology then declines as precipitation is summed
295 over longer periods (Fig. 4a).
296 The high correlation with the single day rainfall totals in late-July coincides with the
297 annual two-week precipitation maximum over eastern Colorado (Fig. 4b). The average two-
298 week precipitation total from July 19-August 1 is higher than every other possible two-week
299 period during the year (e.g., Fig. 4b). On average, nearly 70% of the total precipitation recorded
300 in late-July is contributed by the heaviest single rainfall day in this area (i.e., 68.25%). In fact,
301 when analyzed at the grid point level for eastern Colorado, *all* of the 14-day total can be
302 attributed to a single rain event during some years. The wettest 24 hour period in a given year
303 can occur outside the July 19 to August 1 period, of course, but it is within this 14-day period in
304 late-July when single day precipitation totals tend to be heaviest (Fig. 1) and have the highest
305 correlation with the regional LWa chronology
306 The precipitation response of EW, LW, and RW is strikingly different than LWa in
307 eastern Colorado (Fig. 5). The EW, LW, and RW chronologies have an integrated, nearly annual
308 moisture signal and are most highly correlated with precipitation accumulated over several
309 months prior to and during the growing season. These highest correlations with precipitation for
310 all possible continuous intervals are accumulated over 305, 292, and 308 days during and
311 preceding the growing season for the regional EW, LW, and RW regional chronologies. Using
312 the precipitation response profile for 300-day total precipitation as an example, the highest
313 correlation with both EW and RW is with precipitation totaled from the previous mid-September

to current mid-July (September 22 to July 20, or Julian day 266 of the prior year to day 201 of the current year). The highest 300-day moisture signal for un-adjusted LW is only slightly later (i.e., October 2 to July 31).

The strong relationship between the one-day rainfall totals in midsummer and the regional LWa chronology is present despite the low correlations among the four LWa chronologies. The average correlation among these four chronologies is only r = 0.34 during the calibration period (1947-1997) and r = 0.28 for the full common interval (1779-1997). However, the individual LWa chronologies are more highly correlated with the average gridded time series of the wettest single day in midsummer (range of r = 0.44 to 0.60 for the four chronologies). When these four LWa chronologies are averaged the correlation with the wettest single day time series for eastern Colorado is r = 0.81.

The wettest single day in late-July also tends to be rather weakly correlated among the instrumental rainfall stations [e.g., the four stations closest to the four tree-ring sites and with continuous daily precipitation daily (Denver, Byers, Limon, and Pueblo) are correlated on average at only r = 0.25 for the wettest day at each location from July 19 to August 1, 1948-1997, ranging from r = 0.07 to 0.65]. However, each of these four time series is positively correlated with the wettest single day time series derived from the gridded data (range of r = 0.54 to 0.68 for the four stations). When the daily data are averaged among the four instrumental stations, and the wettest day is identified from this regional average (similar to what presumably happens at the four tree-ring collection sites), the correlation with the wettest single day series based on the gridded data for eastern Colorado improves to r = 0.84. The regional LWa chronology is also highly correlated with the wettest day identified from a regional average of the four stations (r = 0.70).

These comparisons reflect the spatially discontinuous nature of midsummer precipitation events over eastern Colorado, but the common signal between the gridded data (or the weather stations) and the regional LWa chronology can be greatly enhanced with regional averaging. This strong relationship with single-day totals appears to be driven by the extreme years with the highest and lowest single day totals. This is illustrated with a scatterplot between instrumental single day precipitation totals and the normalized regional LWa chronology, highlighting the upper, inter, and lower quartiles from 1948-1997 (Fig. 6a). The correlation between the regional LWa chronology and just the upper and lower quartiles of single day precipitation is strong ($r = 0.88$; Fig. 6a), but the relationship with precipitation in the interquartile range is much weaker ($r = 0.38$; black circles in Fig. 6a). A similar relationship is found when comparing the gridded data and the wettest day based on a four station average of daily precipitation values (Fig. 6b). The correlation with the upper and lower quartiles ($r = 0.90$) is substantially higher compared to values closer to the mean ($r = 0.31$).

The notion that the extreme wet or dry years strongly influence the correlation with the regional LWa chronology is further supported by composites of the 24-hour instrumental totals in the upper and lower quartiles from 1948-1997. The upper quartile composite corresponds with widespread precipitation over most of eastern Colorado and the central Great Plains, resembling frontally organized precipitation (Fig. 6c). This spatial pattern represents thunderstorm activity that might have impacted most if not all of the tree-ring sites used in calculation of the regional LWa chronology. The composite for the lower quartile events indicates that midsummer thunderstorm activity was much less intense across eastern Colorado during these years and late season tree growth would likely have been limited by the lack of precipitation and soil moisture in late-July (Fig. 6d).

360 The reconstruction of late-July one-day rainfall extremes was developed using regression
361 between the LWa chronology (predictor) and the single wettest day from July 19 – August 1 for
362 the eastern Colorado, using the 72 grid point regional average daily data (predictand). The
363 instrumental and the reconstructed values are plotted in Figure 7a. The reconstructed series
364 explains 65% of the interannual variance in one-day rainfall totals during the full 1948-1997
365 calibration period (Fig. 7a). Split calibration and validation experiments on two 25-year sub-
366 periods indicate the relationship between the two series is reasonably stable (Table 1a). The
367 instrumental and reconstructed rainfall distributions are positively skewed by the most extreme
368 wet years (Figs. 7b,c).
369 For comparison with the tree-ring reconstruction, a wettest single day time series
370 computed for midsummer from an average of the four closest rainfall stations was used to
371 develop an alternative 'instrumental-only' regression model. This four-station average of the
372 wettest day in midsummer was regressed with the 72-grid point regional average. The
373 calibration and validation statistics calculated for this experimental instrument-only
374 reconstruction are remarkably similar to the statistics based on the regional tree-ring data (Table
375 1b).
376 The full 241-year time series of reconstructed and instrumental data extends from 1779-
377 2019 (instrumental data only from 1998-2019) and indicates interesting interannual to decadal
378 variability of late-July single day rainfall extremes over eastern Colorado (Fig. 8). The
379 frequency of the wettest >90th percentile events are estimated to have more than doubled from
380 the 19th to 20th centuries, while the driest <10th percentile events appear to have decreased since
381 the late-18th century (Fig. 8). But in spite of the increase in wet extremes, stochastic volatility

382 analysis (Kastner 2016) does not indicate a significant increase in the overall variance of the
383 reconstructed or observed wettest one-day totals (not shown).

384 The late-20th century (1960-1997) is estimated to have experienced a high frequency of
385 one-day rainfall extremes in midsummer (Fig. 8). But there have been only two 90th percentile
386 events since 1998 based on the gridded instrumental data from 1998-2019 (1998 and 2010), and
387 there have been no 10th percentile single day totals over the same period. These changes are also
388 evident in the daily precipitation data recorded at the 40 individual weather stations in eastern
389 Colorado (Fig. 9). Many of the largest events identified in the instrumental data occur between
390 the 1960s and 1990s, and there has been a noticeable decline in the heaviest midsummer
391 precipitation days after 1999.

392 Major sub-decadal to decadal periods of drought identified using instrumental and tree-
393 ring reconstructed PDSI are also apparent in the one-day midsummer rainfall totals (e.g. early-
394 21st century, Seager 2007; 1930s Dust Bowl, Worster 1978; mid-19th century drought;
395 Woodhouse et al. 2002; Herweijer et al. 2006; Cook et al. 2007; Fig. 8). The Dust Bowl Drought
396 in particular had a negative impact on the highest midsummer rainfall totals in eastern Colorado.
397 Eight out of the ten years from 1931-1940 are estimated to have been below average, and the
398 only comparable period of sustained deficits in midsummer single day totals occurred during the
399 1840s and 1850s. The reconstruction of midsummer one-day rainfall is not correlated with a
400 regional average of reconstructed summer PDSI derived from the North American Drought Atlas
401 (Cook et a. 2007) at interannual timescales ($r = 0.07$ from 1779-1997; not shown), but as these
402 major PDSI droughts suggest, prolonged dryness appears to be associated with reduced daily
403 rainfall extremes in midsummer. The decadal estimates of the wettest single day of midsummer
404 time series is also not strongly correlated with decadal estimates of reconstructed PDSI ($r =$

405 0.37), but agreement among these smoothed time series is highest during the most severe and
406 sustained droughts in the regional PDSI reconstructions.

407 The largest instrumental and reconstructed single day extremes during the 1948-1997
408 calibration period represent widespread precipitation events that impact much of eastern
409 Colorado (Fig. 6c), and some of these events were connected with intense flash flooding and
410 severe weather outbreaks. For example, the single day total for July 19, 1985, is the largest
411 estimated event since the late-18th century and is considered one of the wettest days in
412 Colorado's history (Doesken and McKee 1986). Hourly rainfall rates recorded at many stations
413 in eastern Colorado were greater than 25.4 mm on July 19, 1985, and widespread reports of flash
414 flooding and other severe weather hazards including hail, damaging wind, and tornadoes are
415 documented (Doesken and McKee 1986). The reconstructed heavy rainfall day for July 24,
416 1965, was part of a persistent pattern of widespread precipitation from July 20-25, including
417 heavy rains on July 23-24 that led to significant flash flooding of Tucker Gulch in Golden,
418 Colorado. The 1976 Big Thompson Canyon flood and the 1997 Fort Collins event were not
419 identified as extreme single-day events for eastern Colorado in either the instrumental or
420 reconstructed data, but these storms and floods were located north of the study region. It is
421 possible that the heavy one-day rainfall events that led to the flash flooding of Big Thompson
422 and Spring Creek near Fort Collins were recorded in adjusted latewood chronologies of
423 ponderosa pine trees located within or near the vicinity of these drainage basins.

424 The synoptic meteorology of the five largest reconstructed single day rainfall extremes is
425 illustrated in Figure 10. The most common synoptic pattern for these extreme events includes a
426 surface high north of Colorado and a frontal boundary located over the central United States
427 (Figs. 10a,c,e,g,i). Previous flash floods in eastern Colorado have been linked to strong frontal

systems that move south of the region and create post-frontal easterly upslope flow behind the front (Petersen et al. 1999). Precipitable water value anomalies from the surface to 500mb also indicate a deep layer of atmospheric moisture, which tends to increase the efficiency of precipitation (Figs. 10b,d,f,h,j). The 500mb geopotential height patterns vary, but these large precipitation events are often associated with a moderate to strong upper-level ridge over Colorado (Figs. 10b,d,h), or a northwest-tilted ridge that extends from the Great Plains to Pacific Northwest (Figs. 10f,j). The northwest tilted ridge axis (i.e. the bent-back Ridge described by Maddox et al. 1978) has been previously identified as a key upper-level feature for previous flash flooding events in Colorado, including the 1976 Big Thompson Canyon flood and the 1997 flooding of Fort Collins (Maddox et al. 1978; Petersen et al. 1999; Cotton et al. 2003). The general synoptic meteorological features shown in Fig. 10, have been linked to widespread and extreme heavy rainfall over eastern Colorado during the midsummer months (Doswell 1980; Maddox et al. 1980; Petersen et al. 1999; Cotton et al. 2003).

4. Discussion and Conclusions

These results demonstrate that the precipitation response of ponderosa pine tree-ring chronologies can span a large range of time scales, from the annually integrated precipitation signal of total ring width to the daily precipitation extremes recorded by some adjusted latewood width chronologies. The seasonal to annual precipitation signal recorded by total ring-width chronologies has been widely applied, and this long-term integration of climate signal in ring-width data has been the ruling paradigm of dendroclimatology for 100 years (Douglass 1920). However, adjusted latewood width chronologies of ponderosa pine from eastern Colorado are

450 highly correlated with precipitation at the daily timescale and demonstrate the feasibility for the
451 tree-ring reconstruction of weather timescale precipitation totals, or dendrometeorology.
452 The precipitation signals recorded by the last formed latewood cells in ponderosa pine, or
453 other tree species in North America, have not been thoroughly explored. The few studies that
454 have used adjusted latewood chronologies for moisture reconstruction have been calibrated with
455 monthly or seasonal moisture data (e.g., Stahle et al. 2009, 2015; Griffin et al. 2013). Adjusted
456 latewood chronologies also represent just one of several types of tree-ring data that partition the
457 annual growth ring into sub-seasonal timescales. Sub-annual tree-ring data derived with x-ray
458 densitometry (Schweingruber et al. 1978), blue-light intensity (Campbell et al. 2007), or stable
459 isotopes (McCarroll et al. 2014) might potentially record precipitation variability at the daily or
460 weekly time scale, especially in semiarid regions where single events dominate the seasonal
461 totals.
462 In an investigation of more than 300 heavy one day precipitation events for Colorado
463 since the late-19th century, McKee and Doesken (1997) found that extreme rainfall can occur
464 anywhere in Colorado typically from April through October, but there is a distinct peak of
465 occurrence during the last week of July and first few days of August. The heaviest of these
466 events most commonly occur in the foothills just east of the Rocky Mountains. Our results also
467 indicate that the average two week precipitation total from July 19 to August 1 is highest
468 compared to all possible two week intervals for eastern Colorado, and this precipitation maxima
469 is largely the product of heavier single day rainfall totals (Fig. 1). These single day precipitation
470 events, particularly the heaviest days when rainfall is widespread (Fig. 6c), may be the most
471 important source of soil moisture recharge needed for late season tree growth of the ponderosa
472 pine woodlands native to the Rocky Mountain Front Range and foothills of Colorado. Oxygen

473 isotope measurements of the nearly full latewood from mature ponderosa pine in northern
474 Arizona indicate a reliance on winter moisture (Kerhoulas et al. 2017), which is a similar finding
475 to the results shown for the un-adjusted latewood width data in Figure 5. The response to single
476 day rainfall events in midsummer over eastern Colorado was only revealed after using the
477 Kalman Filter to isolate the last-formed xylem cells at the end of the growing season, which are
478 represented by tree-ring chronologies of adjusted latewood width.
479 The reconstruction developed in this study does not estimate the largest single day
480 precipitation totals for the entire year, and in fact there have been a number of extreme
481 precipitation events in Colorado that have led to significant flooding that cannot be captured by
482 ponderosa pine adjusted latewood chronologies (e.g. the event in September 2013). However,
483 the reconstruction does provide a valuable long-term perspective on heavy rains during a two-
484 week interval when extreme rains and severe weather occur with the highest probability (Weaver
485 and Doesken 1990; Mckee and Doesken 1997). The reconstruction estimates that heavy
486 midsummer rainfall events increased from the late-18th century to the late-20th century, with the
487 period from 1960-1997 having the highest frequency of these extremes over the last 241 years.
488 A time series of maximum 24 hour precipitation totals for the entire year based on station
489 observations for Denver from 1872-1993 also seems to indicate that the heaviest 24-hour events
490 for the entire year were on average larger in the mid-to-late 20th century compared to previous
491 periods (McKee and Doesken 1997). Coupled with rapid urban development along the Front
492 Range, some of the heavy rainfall extremes that occurred in midsummer led to costly flash
493 flooding during the late-20th century. Providing a long-term context for the frequency and
494 magnitude of these extreme midsummer precipitation events across many of the vulnerable Front
495 Range drainage basins may now be possible based on the findings of this study. Ponderosa pine

and other semiarid conifer species are native to many of the eastern Rocky Mountain and Front Range drainage basins that have been impacted by severe summer flash flooding, including the Big Thompson Canyon and Spring Creek near Fort Collins. Development of adjusted latewood width chronologies in these vulnerable basins could help investigate changes in the frequency of midsummer precipitation extremes over the last several hundred years.

Acknowledgements

The National Science Foundation funded this study (grant numbers AGS-1266014 and AGS-1702894). We thank Connie Woodhouse and Peter Brown for access to their collections, as well as Ed Cook, Dan Griffin, Dorian Burnette, Song Feng, John Tipton, and Max Torbenson for advice and assistance. We also would like to thank the Mandala Center in Des Moines, New Mexico, for permission to conduct fieldwork.

References

Alexander, M. A., J. D. Scott, K. Mahoney, and J. Barsugli, 2013: Greenhouse gas-induced changes in summer precipitation over Colorado in NARCCAP regional climate models. *J. Clim.*, doi:10.1175/JCLI-D-13-00088.1.

Blasing, T. J., and H. C. Fritts, 1976: Reconstructing past climatic anomalies in the North Pacific and western North America from tree-ring data. *Quat. Res.*, doi:10.1016/0033-5894(76)90027-2.

Campbell, R., D. McCarroll, N. J. Loader, H. Grudd, I. Robertson, and R. Jalkanen, 2007: Blue intensity in Pinus sylvestris tree-rings: Developing a new palaeoclimate proxy. *Holocene*, doi:10.1177/0959683607080523.

Bräuning, A., M. De Ridder, N. Zafirov, I. García-González, D. P. Dimitrov, and H. Gärtner, 2016: Tree-ring features: Indicators of extreme event impacts. *IAWA J.*, doi:10.1163/22941932-20160131.

Barbosa, A. C. M. C., D. W. Stahle, D. J. Burnette, M. C. A. Torbenson, E. R. Cook, M. J. Bunkers, G. Garfin, and R. Villalba, 2019: Meteorological factors associated with frost rings in Rocky Mountain Bristlecone Pine at Mt. Goliath, Colorado. *Tree-Ring Res.*, doi:10.3959/TRR2018-15.

Chen, M., W. Shi, P. Xie, V. B. S. Silva, V. E. Kousky, R. W. Higgins, and J. E. Janowiak, 2008: Assessing objective techniques for gauge-based analyses of global daily precipitation. *J. Geophys. Res. Atmos.*, doi:10.1029/2007JD009132.

Cook, E.R., 1985. A time series analysis approach to tree-ring standardization. Ph.D. Dissertation, University of Arizona, 171 pp.

Cook, E.R., and Paul J. Krusic, 2005: Program ARSTAN: A Tree-ring Standardization Program Based on Detrending and Autoregressive Time Series Modeling with Interactive Graphics

Lamont-Doherty Earth Observatory, Columbia University, Palisades, NY

Cook, E. R., L. A. Kairiukstis, C. E.R., and L. A. Kairiukstis, 1990: Methods of Dendrochronology. Kluwer Academic Publishers, Boston.

Cook, E. R., R. Seager, M. A. Cane, and D. W. Stahle, 2007: North American drought: Reconstructions, causes, and consequences. *Earth-Science Rev.*, doi:10.1016/j.earscirev.2006.12.002.

Cook E.R., P.J. Krusic, and T.M. Melvin, 2014: Program RCSigFree. Tree-Ring Lab, Lamont Doherty Earth Observatory of Columbia University, Palisades, NY.

Cotton, W. R., R. L. McAnelly, and T. Ashby, 2003: Development of new methodologies for determining extreme rainfall: Final report for contract ENC #C154213. Dept. of Natural Resources, State of Colorado, 140 pp. [Available online at http:// rams.atmos.colostate.edu/precip-proj/reports/022003/DNR_ Final_report.pdf.]

Crawford, C. J., D. Griffin, and K. F. Kipfmueller, 2015: Capturing season-specific precipitation signals in the northern Rocky Mountains, USA, using earlywood and latewood tree rings. J. Geophys. Res. Biogeosciences, doi:10.1002/2014JG002740.

Dannenberg, M. P., and E. K. Wise, 2016: Seasonal climate signals from multiple tree ring metrics: A case study of Pinus ponderosa in the upper Columbia River Basin. *J. Geophys. Res. Biogeosciences*, doi:10.1002/2015JG003155.

Doesken, N.J., and T.B. McKee, 1986: Colorado Climate water-year series (October 1 1984-September 1985). Climo Rpt 86-1, Dept. of Atmos. Sci., CSU, Fort Collins, CO, June, 115 pp.

554 Doesken, N.J., and T.B. McKee, 1998: An Analysis of Rainfall for the July 28, 1997 Flood in
555 Fort Collins, Colorado. Climatology Report 98-1, Dept. of Atmos. Sci., CSU, Fort Collins, CO,
556 February, 55 pp.
557 Doswell, C. A., 1980: Synoptic-Scale Environments Associated with High Plains Severe
558 Thunderstorms. *Bull. Am. Meteorol. Soc.*, doi:10.1175/1520-
559 0477(1980)061<1388:sseawh>2.0.co;2.
560 Douglass, A. E., 1920: Evidence of Climatic Effects in the Annual Rings of Trees. *Ecology*,
561 doi:10.2307/1929253.
562 Draper, N., and H. Smith, 1981: Applied regression analysis 2nd ed. *Technometrics*,
563 doi:10.1198/tech.2005.s303.
564 Edmondson, J. R., 2010: The Meteorological Significance of False Rings in Eastern Redcedar
565 (Juniperus virginiana L.) from the Southern Great Plains, U.S.A. *Tree-Ring Res.*,
566 doi:10.3959/2008-13.1.
567 Fritts H.C., 2001: Tree rings and climate. Blackburn Press, Clarendan
568 Gochis, D., and Coauthors, 2015: The great Colorado flood of September 2013. *Bull. Am.*
569 *Meteorol. Soc.*, doi:10.1175/BAMS-D-13-00241.1.
570 Griffin, D., D. M. Meko, R. Touchan, S. W. Leavitt, and C. A. Woodhouse, 2011: Latewood
571 Chronology Development for Summer-Moisture Reconstruction In the US Southwest. *Tree-Ring*
572 *Res.*, doi:10.3959/2011-4.1.
573 Griffin, D., and Coauthors, 2013: North American monsoon precipitation reconstructed from
574 tree-ring latewood. *Geophys. Res. Lett.*, doi:10.1002/grl.50184.
575 Hales, J. E., 1974: Southwestern United States Summer Monsoon Source—Gulf of Mexico or
576 Pacific Ocean? *J. Appl. Meteorol.*, doi:10.1175/1520-0450(1974)013<0331:sussms>2.0.co;2.

577 Herweijer, C., R. Seager, and E. R. Cook, 2006: North American droughts of the mid to late
578 nineteenth century: A history, simulation and implication for Mediaeval drought. *Holocene*,
579 doi:10.1191/0959683606hl917rp.
580 Hoaglin, D.C., F. Mosteller, and J.W. Tukey, 2000: Understanding Robust and Exploratory Data
581 Analysis. Wiley, 447 pp.
582 Hoerling, M. P., and Coauthors, 2013: Present weather and climate: Evolving conditions.
583 *Assessment of Climate Change in the Southwest United States: A Report Prepared for the*
584 *National Climate Assessment*.
585 Howard, I. M., D. W. Stahle, and S. Feng, 2019: Separate tree-ring reconstructions of spring and
586 summer moisture in the northern and southern Great Plains. *Clim. Dyn.*, doi:10.1007/s00382-
587 018-4485-8.
588 Kalnay, E., and Coauthors, 1996: The NCEP/NCAR 40-year reanalysis project. *Bull. Am.*
589 *Meteorol. Soc.*, doi:10.1175/1520-0477(1996)077<0437:TNYRP>2.0.CO;2.
590 Karl, T. R., and R. W. Knight, 1998: Secular Trends of Precipitation Amount, Frequency, and
591 Intensity in the United States. *Bull. Am. Meteorol. Soc.*, doi:10.1175/1520-
592 0477(1998)079<0231:STOPAF>2.0.CO;2.
593 Kastner, G., 2016: Dealing with Stochastic Volatility in Time Series Using the R Package
594 stochvol . *J. Stat. Softw.*, doi:10.18637/jss.v069.i05.
595 Kerhoulas, L.P., T.E. Kolb, and G.W. Koch, 2017: The influence of monsoon climate on
596 latewood growth of southwestern ponderosa pine. *Forests*, doi: 10.3390/f8050140
597 Kunkel, K. E., L. E. Stevens, S. E. Stevens, L. Sun, E. Anssen, D. Wuebbles, K. T. Redmond,
598 and J. G. Dobson, 2013: Regional Climate Trends and Scenarios for the U.S. National Climate
599 Assessment. *NOAA Tech. Rep. NESDIS*.

LaMarche, V. C., and K. K. Hirschboeck, 1984: Frost rings in trees as records of major volcanic eruptions. *Nature*, doi:10.1038/307121a0.

Lukas J., Barsugli J., Doesken, N., Rangwala, I., and K. Wolter, 2014: Climate change in Colorado: a synthesis to support water resources management and adaptation. *A Report for the Colorado Water Conservation Board, Western Water Assessment*, 114 pp.

Maddox, R. A., L. R. Hoxit, C. F. Chappell, and F. Caracena, 1978: Comparison of Meteorological Aspects of the Big Thompson and Rapid City Flash Floods. *Mon. Weather Rev.*, doi:10.1175/1520-0493(1978)106<0375:comaot>2.0.co;2.

Maddox, R. A., F. Canova, and L. R. Hoxit, 1980: Meteorological Characteristics of Flash Flood Events over the Western United States. *Mon. Weather Rev.*, doi:10.1175/1520-0493(1980)108<1866:mcoffe>2.0.co;2.

Mahoney, K., F. M. Ralph, K. Wolter, N. Doesken, M. Dettinger, D. Gottas, T. Coleman, and A. White, 2014: Climatology of Extreme Daily Precipitation in Colorado and Its Diverse Spatial and Seasonal Variability. *J. Hydrometeorol.*, doi:10.1175/jhm-d-14-0112.1.

Mahoney, K.M., Lukas, J.J., and M. Mueller, 2018: Colorado – New Mexico Regional Extreme Precipitation Study Summary Report, Volume VI: Considering Climate Change in the Estimation of Extreme Precipitation for Dam Safety. *MONOGRAPH - Technical Report. CO Division of Water Resources and NM Office of the State Engineer*

Matthai, H.F., 1969. Floods of June 1965 in South Platte River Basin Colorado. *Water Supply Paper 1850 – B*. US Geological Survey, Washington DC.

McCarroll, D., and N. J. Loader, 2004: Stable isotopes in tree rings. *Quaternary Science Reviews*.

McKee, T. B., and N. J. Doesken, 1997: Colorado Extreme Storm Precipitation Data Study:

623 Final report. Climatology Rep. 97-1, Dept. of Atmospheric Science, Colorado State
624 University, Fort Collins, CO, 109 pp. [Available online at http://ccc.atmos.
625 colostate.edu/pdfs/Climo_97-1_Extreme_ppt.pdf.]
626 Meko, D. M., 1981: Applications of Box-Jenkins methods of time series analysis to the n
627 reconstruction of drought from tree rings. Ph.D. dissertation, The University of Arizona, 149 pp.
628 Meko, D. M., and C. H. Baisan, 2001: Pilot study of latewood-width of conifers as an indicator
629 of variability of summer rainfall in the North American monsoon region. *Int. J. Climatol.*,
630 doi:10.1002/joc.646.
631 Melvin, T. M., and K. R. Briffa, 2008: A "signal-free" approach to dendroclimatic
632 standardisation. *Dendrochronologia*, doi:10.1016/j.dendro.2007.12.001.
633 Palmer, W. C., 1965: Meteorological Drought. *U.S. Weather Bur. Res. Pap. No. 45*,.
634 Petersen, W. A., and Coauthors, 1999: Mesoscale and radar observations of the Fort Collins flash
635 flood of 28 July 1997. *Bull. Am. Meteorol. Soc.*, doi:10.1175/1520-
636 0477(1999)080<0191:MAROOT>2.0.CO;2.
637 Schweingruber, F., H. Fritts, O. Braker, L. Drew, and E. Schar, 1978: The X-ray technique as
638 applied to dendroclimatology. *Tree-Ring Bull*. 38, 61–91.
639 Stahle, D.W., 1990: The tree-ring record of false spring in the southcentral United States. Ph.D.
640 Dissertation, Arizona State University, 272 pp.
641 Stahle, D. W., and M. K. Cleaveland, 1992: Reconstruction and Analysis of Spring Rainfall over
642 the Southeastern U.S. for the Past 1000 Years. *Bull. Am. Meteorol. Soc.*, doi:10.1175/1520-
643 0477(1992)073<1947:raaosr>2.0.co;2.
644 Stahle, D. W., and Coauthors, 2009: Cool- and warm-season precipitation reconstructions over
645 western New Mexico. *J. Clim.*, doi:10.1175/2008JCLI2752.1.

Stahle, D. W., J. R. Edmondson, J. N. Burns, D. K. Stahle, D. J. Burnette, E. Kvamme, C. Lequesne, and M. D. Therrell, 2015: Bridging the Gap With Subfossil Douglas-Fir At Mesa Verde, Colorado. *Tree-Ring Res.*, doi:10.3959/1536-1098-71.2.53.

Tang, M., and E. R. Reiter, 1984: Plateau Monsoons of the Northern Hemisphere: A Comparison between North America and Tibet. *Mon. Weather Rev.*, doi:10.1175/1520-0493(1984)112<0617:pmotnh>2.0.co;2.

Torbenson, M. C. A., D. W. Stahle, J. Villanueva Díaz, E. R. Cook, and D. Griffin, 2016: The Relationship Between Earlywood and Latewood Ring-Growth Across North America. *Tree-Ring Res.*, doi:10.3959/1536-1098-72.02.53.

Villalba, R., and T. Veblen, 1996: A tree-ring record of dry spring-wet summer events in the forest-steppe ecotone, northern Patagonia, Argentina. *Tree Rings, Environ. Humanit.*,.

Weaver, J. F., and N. J. Doesken, 1990: Recurrence probability – a different approach. *Weather*, doi:10.1002/j.1477-8696.1990.tb05659.x.

Welch, G., and G. Bishop, 2006: An Introduction to the Kalman Filter. *In Pract.*, doi:10.1.1.117.6808.

Wells, P. V., 1965: Scarp woodlands, transported grassland soils, and concept of grassland climate in the great plains region. *Science*, doi:10.1126/science.148.3667.246.

Woodhouse, C. A., and P. M. Brown, 2001: Tree-ring evidence for Great Plains drought. *Tree-Ring Res.,* 57, 89-103.

Woodhouse, C. A., J. J. Lukas, and P. M. Brown, 2002: Drought in the western Great Plains, 1845-56. Impacts and implications. *Bull. Am. Meteorol. Soc.*, doi: 10.1175/BAMS-83-10-1485

Woodhouse, C. A., and J. J. Lukas, 2006: Drought, Tree Rings and Water Resource Management in Colorado. *Can. Water Resour. J.*, doi:10.4296/cwrj3104297.

669 Worster, D., 1979. Dust Bowl. The Southern Plains in the 1930s. Oxford University Press, 304
670 pp.
671 Wuebbles, D. J., and Coauthors, 2017: *Executive summary. Climate Science Special Report:*
672 *Fourth National Climate Assessment, Volume I*.
673 Xie, P., M. Chen, S. Yang, A. Yatagai, T. Hayasaka, Y. Fukushima, and C. Liu, 2007: A Gauge-
674 Based Analysis of Daily Precipitation over East Asia. *J. Hydrometeorol.*, doi:10.1175/jhm583.1
675

Table 1 The calibration and validation statistics computed for the tree-ring reconstruction of one-day precipitation totals in late-July over eastern Colorado are listed (a). The same statistics for an experimental reconstruction using an average of the largest one-day rainfall totals among the four weather stations closest to the tree-ring collection sites are also listed (b; Byers, Denver, Limon, Pueblo; July 19 to August 1). The statistics include the coefficient of determination, R^2, adjusted downward for loss of degrees of freedom (Draper and Smith 1981); the Pearson product moment correlation coefficient, r (Draper and Smith 1981), reduction of error, RE (Fritts 2001); coefficient of efficiency, CE, and the root mean square error (RMSE; Cook and Kairiukstis 1990).

a. Regional LWa chronology

Calibration Period	Adj. R^2	Validation Period	r	RE	CE	RMSE
1973-1997	0.75	1948-1972	0.75	0.51	0.49	11.00
1948-1972	0.55	1973-1997	0.87	0.71	0.70	11.28
1948-1997	0.65	----------	-----	------	-----	11.25

b. Four station single day precipitation totals in late-July

Calibration Period	Adj. R^2	Validation Period	r	RE	CE
1973-1997	0.73	1948-1972	0.78	0.66	0.59
1948-1972	0.59	1973-1997	0.86	0.74	0.72
1948-1997	0.70	----------	-----	------	-----

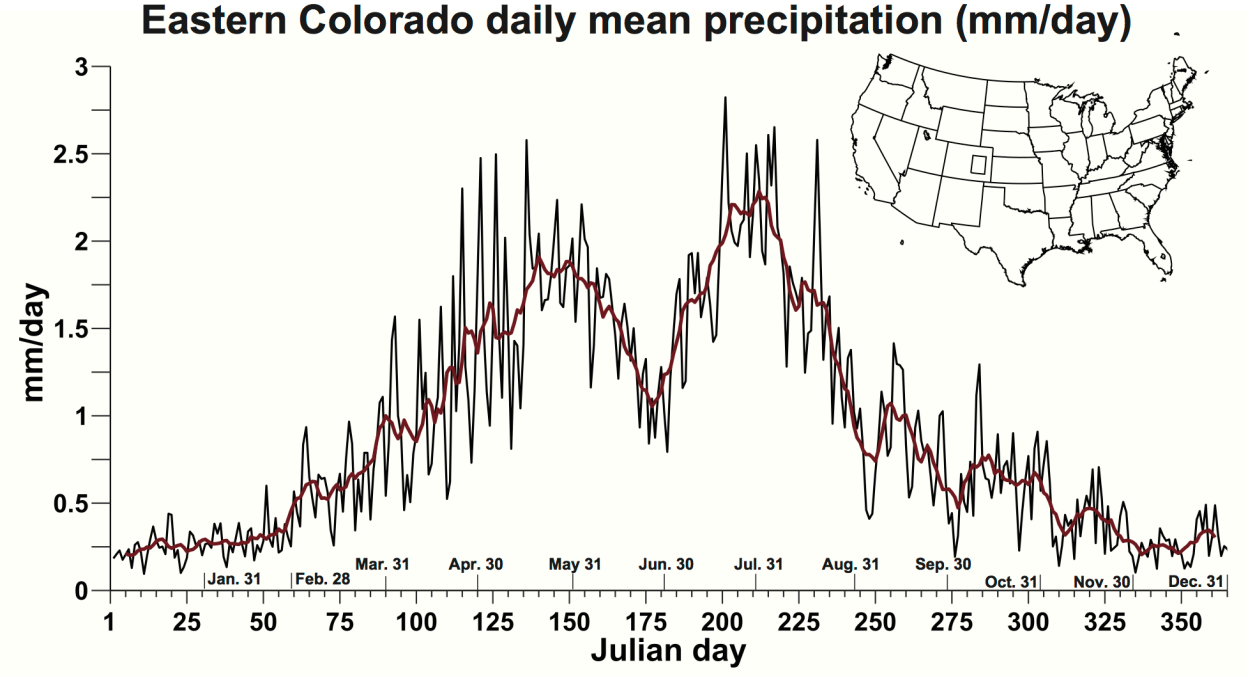

686

687 **Fig. 1** The daily mean precipitation totals for 1948-2019 are plotted for a regional average of

688 eastern Colorado from the CPC 0.25°x0.25° Daily U.S. Unified Gauge-Based Analysis of

689 Precipitation dataset [37.75°-39.75N°, 105°-103°W; black box on the map inset]. The red line is

690 a 10-day moving average of the daily means. Note the two peaks in the climatology of daily

691 rainfall during late-spring and midsummer.

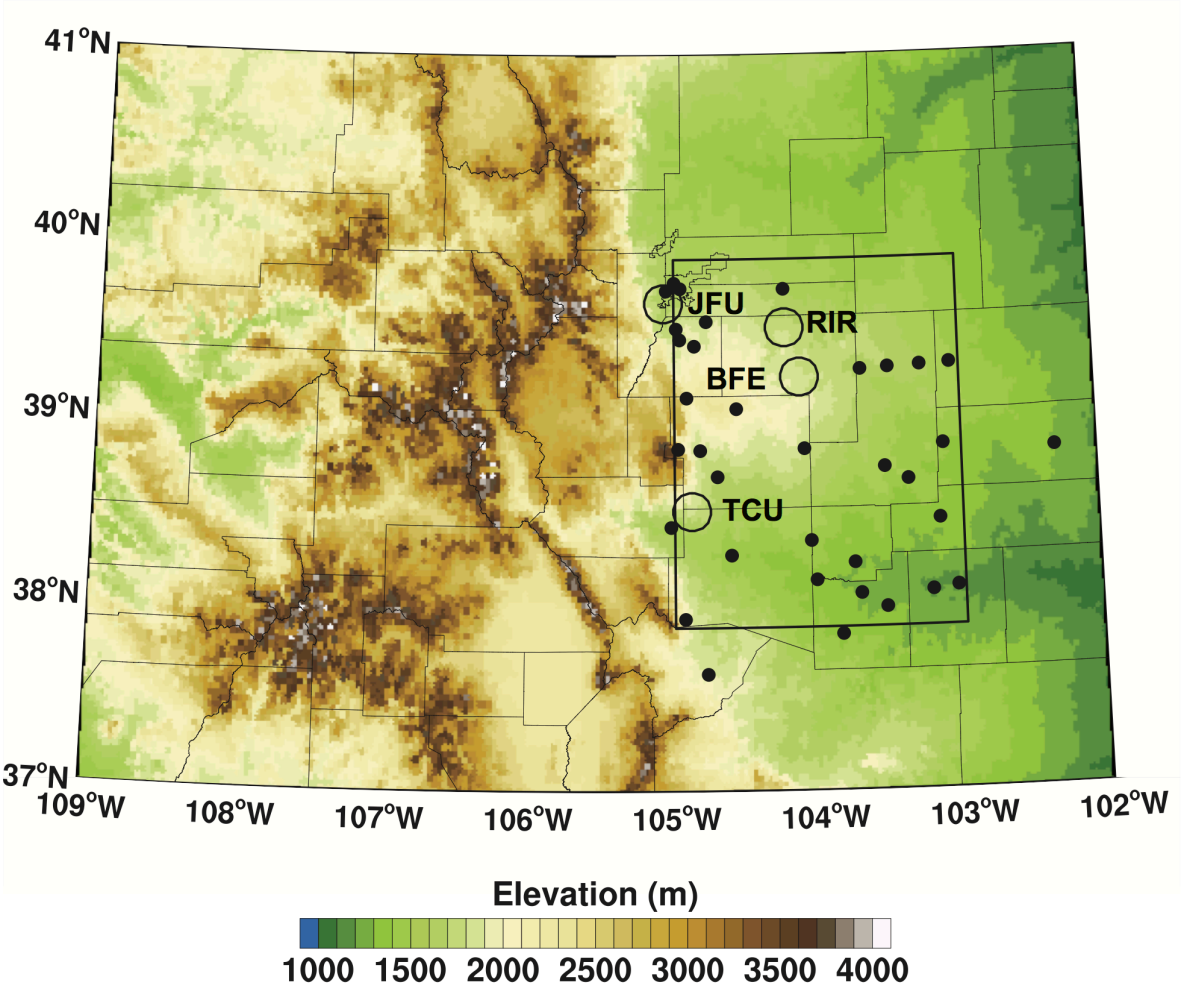

692

693 **Fig. 2** This map locates the ponderosa pine stands used to develop the adjusted latewood width

694 chronologies (open circles labeled BFE, JFU, RIR, TCU and defined in text). The black dots are

695 the locations of the 40 instrumental precipitation stations. The box outlines the study area where

696 the 72 grid points were used to compute the regional average daily precipitation totals for eastern

697 Colorado.

698

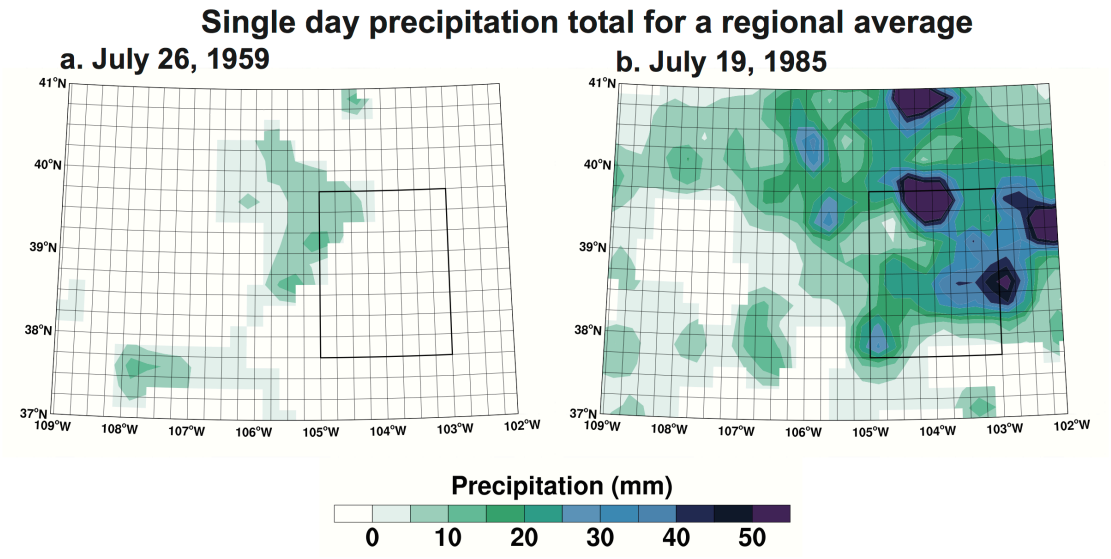

699

700 **Fig. 3** These maps illustrate two different examples of the *wettest single day precipitation total*
701 during the 14-day interval from July 19 to August 1 for (a) 1959 and (b) 1985. The precipitation
702 totals calculated from the 72 grid point regional average of the daily data were 1.35 mm and
703 25.67 mm for July 26, 1959 and July 19, 1985, respectively. These wettest days were identified
704 each year to derive the annual time series of the single wettest day occurring in late-July for
705 eastern Colorado.

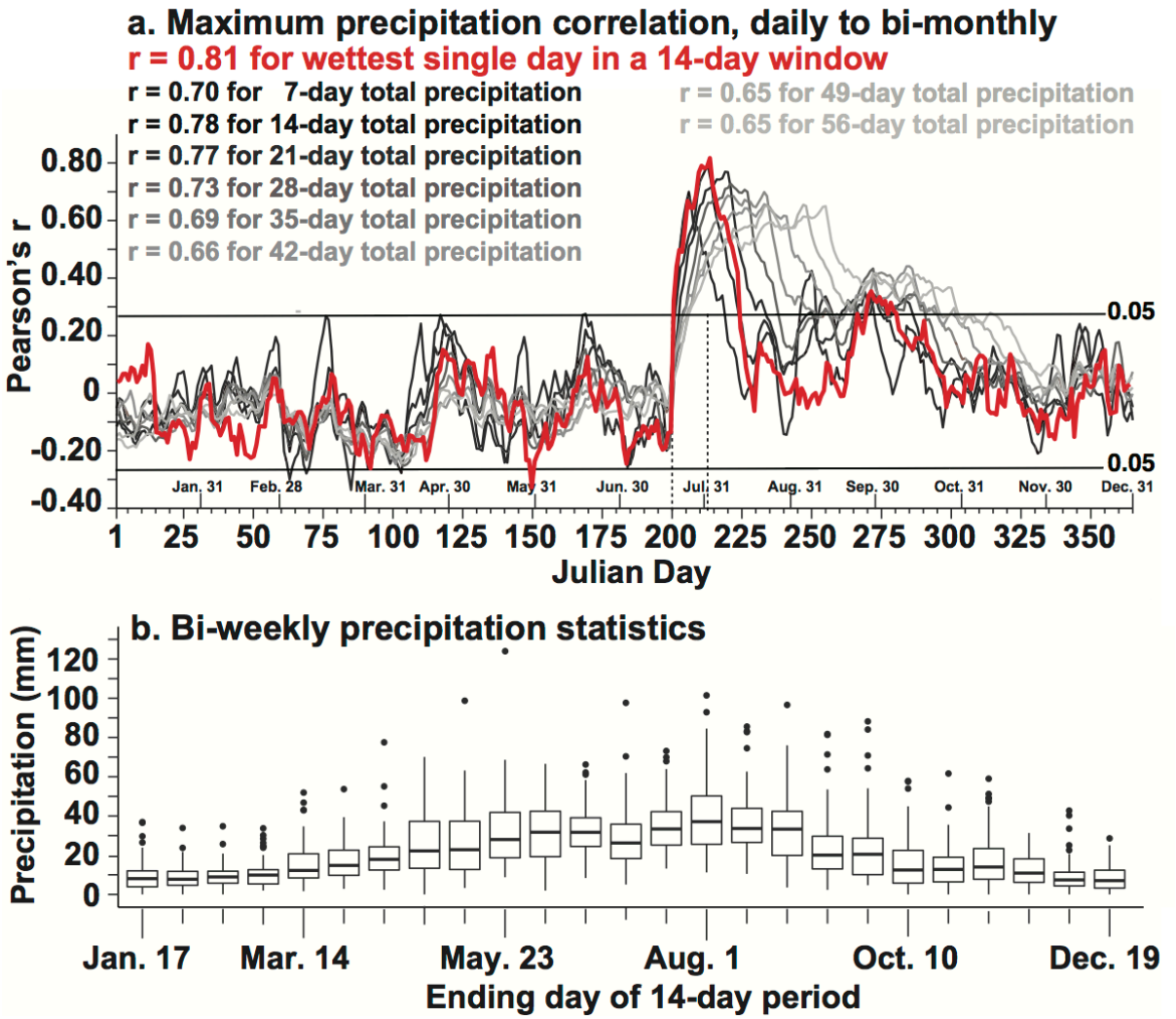

706

707 **Fig. 4** (a) The correlations between the regional LWa chronology and the *wettest single day*

708 *precipitation total* over the eastern Colorado study area during overlapping 14-day intervals (i.e.

709 each period overlaps the previous by 13 days) from 1948-1997 are plotted by Julian date of the

710 year (red line; significance thresholds noted). The highest correlation was computed for the

711 wettest daily total during the 14-day interval extending from Julian day 200 to 213 (July 19 to

712 August 1; r = 0.81). The vertical dashed lines denote this best 14-day interval (correlations are

713 plotted at the end date of each 14-day interval). The correlation between the regional LWa

714 chronology and precipitation *totals* accumulated for all possible 7 to 56 day periods during the

715 year are also plotted (gray scale). The highest LWa correlation with 14-day *total* rainfall is also

716 from Julian day 200 to 213 (r = 0.78), but is still below the correlation with the single wettest day
717 during this interval (r = 0.81). (b) Box and whisker plots of the non-overlapping bi-weekly
718 precipitation climatology for the study area. The mean, upper, and lower quartiles are plotted in
719 each box, along with the highest extreme values (dots; 1948-2019). Note that the highest two-
720 week mean precipitation also corresponds with the two-week interval in (a) when the regional
721 LWa chronology is most highly correlated with daily precipitation (i.e., late-July).
722
723

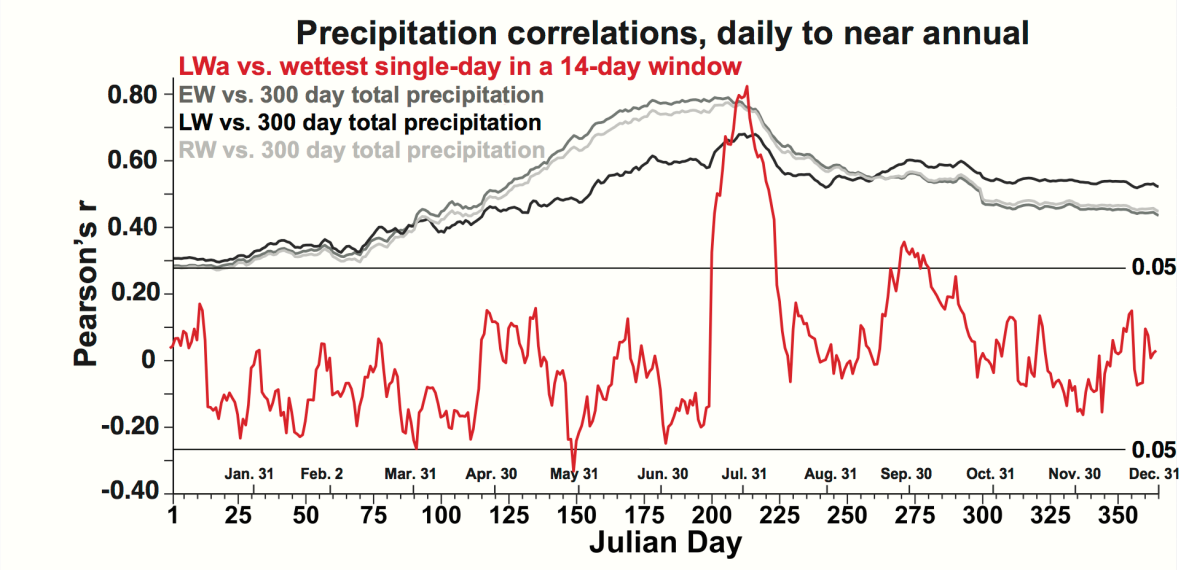

724

725 **Fig. 5** The correlation of the regional LWa chronology with the wettest single day in all possible
726 overlapping 14-day intervals from 1948-1997 peaks in late-July (red line; from Fig. 4a) and is
727 compared with the correlations between the regional chronologies of EW, LW, and RW for
728 eastern Colorado for all possible continuous 300-day precipitation totals throughout the year
729 (gray scale lines). The gridded daily precipitation data were totaled for all 300-day intervals
730 beginning in the previous year and ending on the Julian date noted on the x-axis during the
731 current year for 1948-1997 (January 1 = previous Julian day 66 to current day 1). Note the
732 strong near-annual precipitation signals integrated in the EW, LW, and RW chronologies, all of
733 which include significant correlations during winter, spring, and summer. However, the LWa
734 chronology is strongly correlated with single day precipitation totals only in late-July.

735

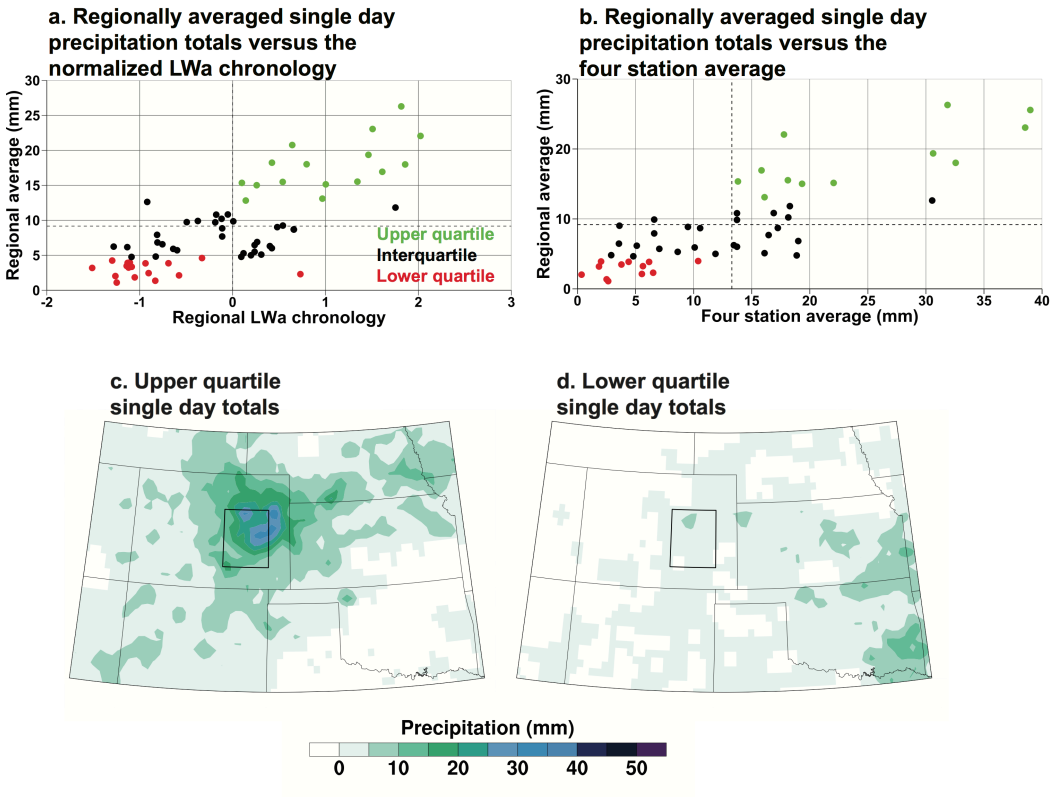

736

737 **Fig. 6** (a) This scatterplot between instrumental single day precipitation totals and the
738 normalized LWa chronology for eastern Colorado illustrates the importance of rainfall extremes
739 in the upper and lower quartiles [upper quartile (green), interquartile (black), and the lower
740 quartile (red)]. (b) Same as (a) using the wettest day identified in the instrumental four-station
741 average of daily precipitation totals as the dependent variable. The instrumental precipitation
742 totals are averaged for the upper (c; n = 13) and the lower quartile events (d; n = 12) for late-July
743 from 1948-1997.

744

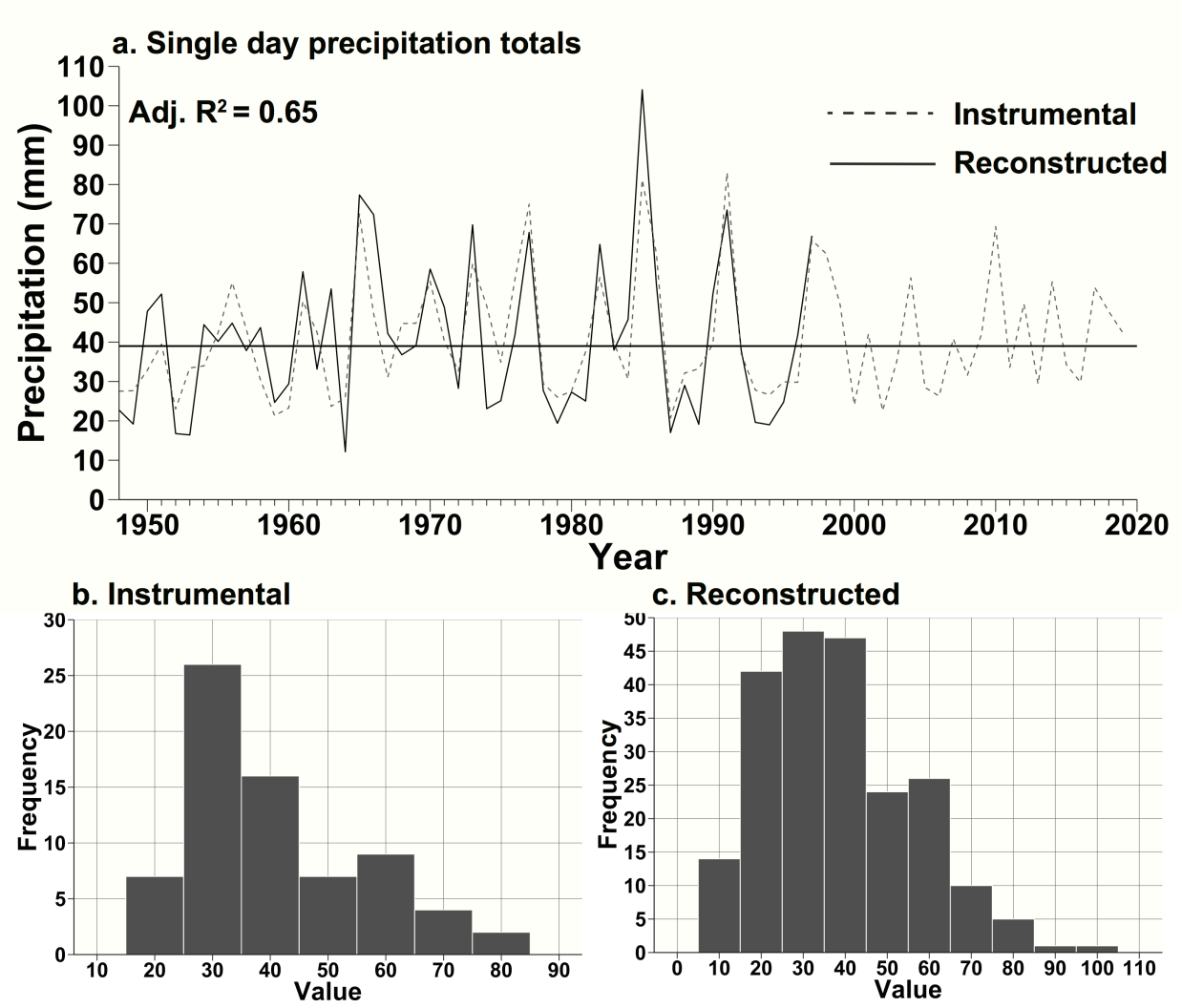

745

746 **Fig. 7** (a) The instrumental and reconstructed highest single day precipitation totals in late-July
747 are plotted from 1948-1997 (1998-2019 is instrumental data only for the 72 grid point regional
748 average; instrumental mean also plotted). The reconstructed series are estimates after the
749 variance lost in the regression has been restored. The frequency distributions of the instrumental
750 (b) and reconstructed (c) highest single day totals in late-July are also illustrated, based on the
751 periods 1948-2019 and 1779-1997, respectively.

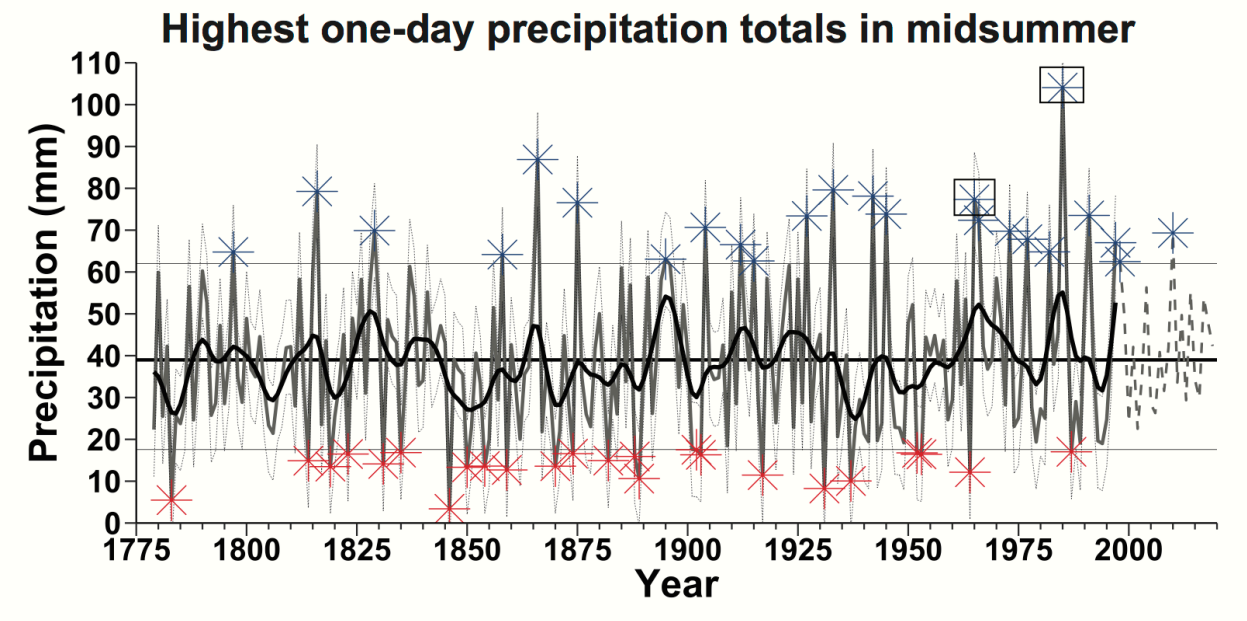

752

753 **Fig. 8** The highest one-day precipitation totals in midsummer were reconstructed from 1779-
754 1997 (gray) and the instrumental data were appended from 1998-2019 (dashed). The full 1779-
755 2019 time series is not a single homogenous time series given the reconstruction contains
756 uncertainty. Uncertainty is estimated based on the 80% confidence interval of the root mean
757 square error (light gray lines; Table 1a). A smoothed version of the reconstruction that
758 highlights decadal variability is plotted in black from 1779-1997. The mean, 90th, and 10th
759 percentile thresholds for 1779-2019 are plotted and extremes above or below these thresholds are
760 noted (asterisks). Heavy precipitation days that were associated with significant flash flooding
761 and severe weather in Colorado on July 24, 1965 and July 19, 1985 are also indicated (squares).

762

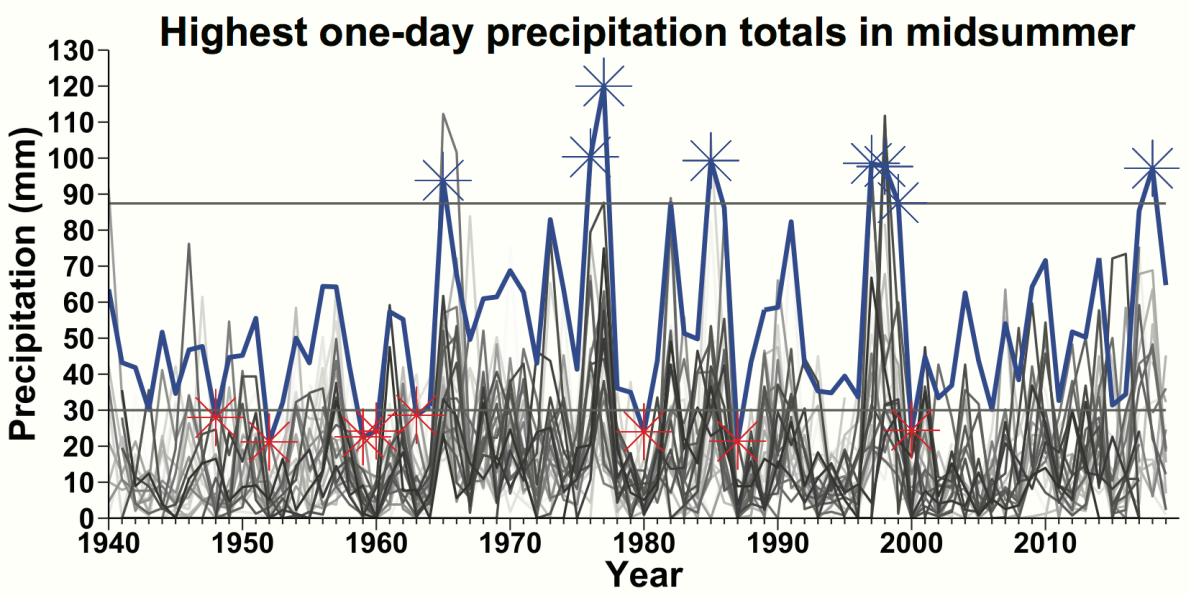

763

764 **Fig. 9** The highest single day precipitation totals identified at the 40 instrumental weather
765 stations during midsummer are plotted individually from 1948-2019 (i.e., July 19 to August 1;
766 gray scale). A time series of the wettest day based on an average of the daily data for the 40
767 stations is also plotted (thick blue line) after being rescaled to the time series of the highest daily
768 precipitation total identified from all 40 stations each year. Extremes above or below the 90th
769 and 10th percentile thresholds are indicated for the regional average (asterisks).

770

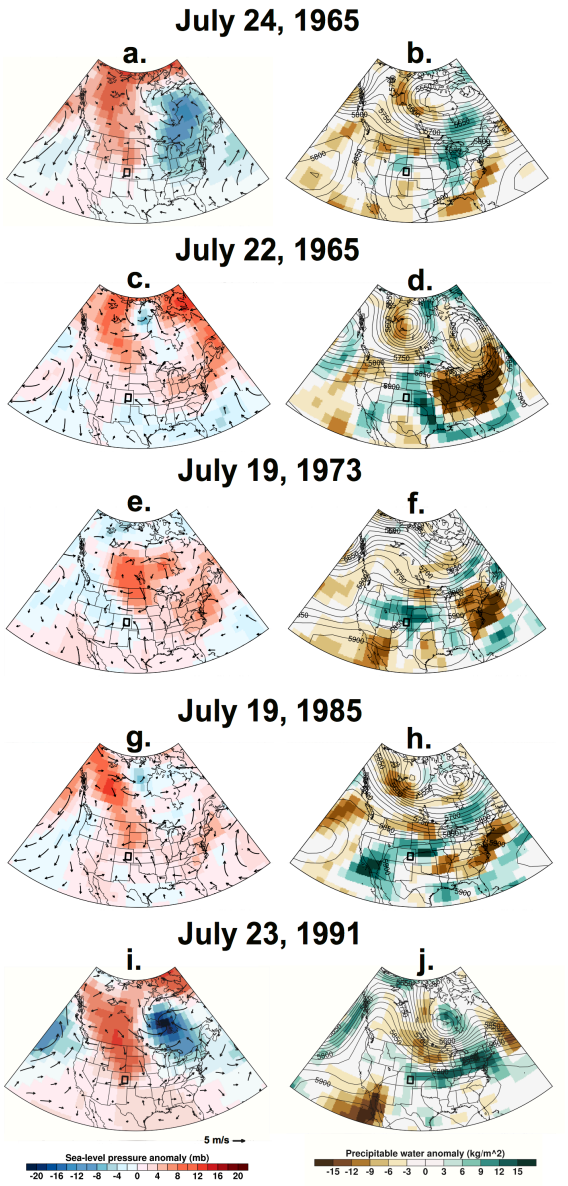

771

772 **Fig. 10** The surface pressure anomaly (mb; shaded) and surface wind speed and direction (m/s;
773 wind vectors) for the five highest reconstructed single day precipitation totals in midsummer
774 from 1948-1997 are shown for (a) July 24, 1965, (c) July 22, 1966, (e) July 19, 1973, (g) July 19,
775 1985, (i) July 23, 1991. Note the large region of anomalous high pressure north of Colorado
776 extending into Canada, and the area of low level wind convergence over the central United States
777 for all events. (b,d,f,h,j) Mean 500mb geopotential heights (contours) and the precipitable water

778 value anomalies (kg/m^2) calculated from the surface to 500mb are mapped for these five most

779 extreme wet days of midsummer.

780
781